International Journal of Thermal Sciences 171 (2022) 107196

Contents lists available at ScienceDirect

International Journal of Thermal Sciences

journal homepage: www.elsevier.com/locate/ijts

Analytical and numerical approach to convective heat transfer through a granular target with gas cooling

P. Cupiał, Ł. Łacny *, J. Snamina

AGH University of Science and Technology, Faculty of Mechanical Engineering and Robotics, al. Mickiewicza 30, Krakow, Poland

ARTICLE INFO

Keywords:
Heat transfer
Packed bed target
Helium cooling
Porous medium
Accelerator technology

ABSTRACT

The paper presents an analytical and a numerical approach to studying the effectiveness of the cooling of a granular target by gaseous helium. The increase in the target temperature is caused by an impinging beam which deposits a very high power of 138 kW inside the limited volume of the target. A porous domain approach is used to model the flow of helium through the packed-bed target. An efficient one-dimensional analytical model is proposed to describe the transverse flow of gas helium, which accounts for its compressibility and the heat exchange between the target spheres and the cooling gas. The predictions of this model are shown to be in good agreement with more complex numerical studies done with Fluent.

1. Introduction

The design of high-power targets constitutes a challenging issue in high-energy physics experiments. Such targets are struck by particle beams with an average power that can exceed 1 MW. A substantial part of this power is released as heat in the target, so that efficient target cooling is a very important issue. Apart from solid targets, e.g. made of graphite, the use of a packed-bed of small spheres may provide a viable solution. An early concept of such a target was proposed in [1], which includes an interesting general discussion of the potential of this design. Some computational fluid dynamics (CFD) results can be found in [2]. The main advantages of a packed-bed design are that due to its granular structure, the stress level is reduced compared to solid targets, and efficient gas cooling is possible by means of a medium flowing through the target pores. Thanks to these advantages a packed-bed design is now being considered for the ESSνSB experiment, the potential physics reach of which is described in [3].

In this paper an efficient one-dimensional analytical model is described, which allows for an assessment of the cooling of a packed-bed target, with little computational effort. Both the gas flow through a porous medium and heat exchange between the spheres and the cooling gas have been modelled. An important element of this study is the analysis of the steady-state operation of the target under a sequence of very short proton beam pulses, which to the authors' best knowledge is new. The results obtained using the analytical model are shown to be in good agreement with CFD results, which are computationally much more demanding.

Compressible fluid flow through a porous medium, which does not account for the heat exchange between the flowing gas, has been studied, e.g., in [4–7]. Ergun's semi-empirical formula is very often applied to model gas flow through such a medium, which will also be used in the present study. Heat exchange for packed-beds has earlier been described, e.g., in [4,8,9]. The application to the analysis of a packed bed gas-cooled nuclear reactor has been described in [10].

The model developed in this paper can be used to study the effect of various parameters, such as the packing ratio, different materials of the spheres or the gas flow conditions, on the temperature inside the target, which is of much importance in the design process.

2. Model description

The granular target considered in this study is a rod of length $L_t = 0.78$ m and diameter $D_t = 0.03$ m, consisting of titanium spheres of mean diameter $d = 3 \times 10^{-3}$ m. A model of the target with inlet and outlet slots is shown in Fig. 1. It is assumed for the purpose of the present study, that the porosity of the target is equal to $\epsilon = 0.34$, so that 66% of the target consists of titanium alloy spheres, while the space in between the spheres is filled with the coolant (gaseous helium).

During the ESSνSB experiment, the purpose of which is the production of an intense neutrino super beam [3], a 5 MW proton beam ($E_{p+} = 2.5$ GeV) from the linear accelerator at the European Spallation Source at Lund (Sweden), will be split laterally into four 1.25 MW beams, each of which striking a separate target placed inside a magnetic horn. The impinging proton beam will consist of 1.3 μs proton pulses repeated at a frequency of $f = 14$ Hz. As a result of the interaction of the beam with the target spheres, and assuming that the spheres are made of titanium,

* Corresponding author.
E-mail address: llacny@agh.edu.pl (Ł. Łacny).

https://doi.org/10.1016/j.ijthermalsci.2021.107196
Received 4 December 2020; Received in revised form 21 June 2021; Accepted 24 July 2021
Available online 7 August 2021

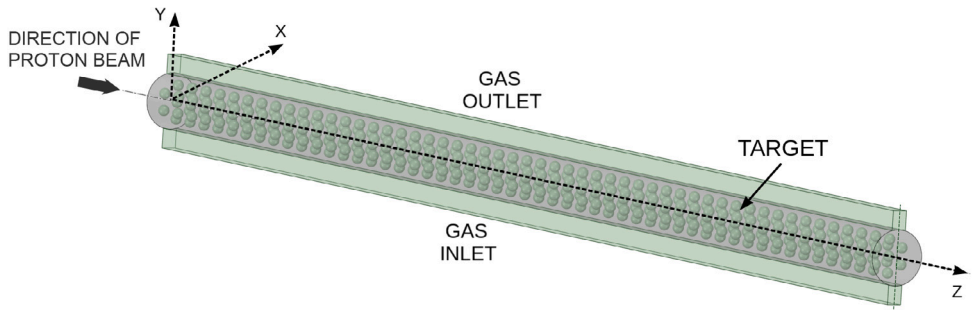

Fig. 1. 3-dimensional model of the target with inlet slot at the bottom and outlet slot at top, along the whole length of the target.

an estimated 138 kW will be dissipated in the target as heat. Efficient heat removal from the target becomes therefore a very important issue.

The heat energy is deposited by the beam inside the spheres over a short time of about 1 μs at the beginning of each cycle, and afterwards transferred to the surrounding medium over the rest of the cycle ($t_c = 1/f = 0.071$ s), in accordance with the known laws of heat transfer. The principal mechanism is the transmission of heat from the surface of the spheres to the helium flowing outside, known as forced heat convection. The dissipation of heat from the spheres is also caused by radiation, heat conduction between the spheres themselves at the points of contact and heat conduction between the spheres and the casing (for the spheres in touch with the inner surface of the target shell).

Because of the amount of energy released in the titanium spheres, a large helium mass flow rate is required. Pushing such a big amount of gas through the target in the axial direction is not feasible due to both its length and small diameter, but especially due to the high sphere-packing ratio inside the target. This is the main reason for selecting transverse target cooling via the introduction of two slots (inlet & outlet) located on the perimeter, on the opposite sides of the target, as shown in Fig. 1.

3. Analytical approach

In the analytical model of heat transfer inside the granular target the assumption is made that for a given longitudinal z-coordinate the temperature, pressure and velocity of helium are functions of only the y-coordinate. In addition, the solution is obtained for the steady-state condition, when the balance between the heat introduced into the system and the heat absorbed by the flowing gas is reached.

3.1. Properties of helium under considerable temperature and pressure change

Under the changing pressure and thermal conditions the properties of helium also change. When determining the heat transfer coefficient between the titanium spheres and the flowing helium, it is essential to consider both the dynamic viscosity and thermal conductivity of helium. Experimental data shows that both these coefficients are strongly dependent on temperature and only slightly on pressure. In practical applications, semi-empirical equations that specify the dynamic viscosity and thermal conductivity of a gas can be used. Based on [11], the following equations, which hold true within the pressure range from 1 to 100 bar and from the room temperature of about ~ 293 K up to 1800 K, are used in the present study:

$$\mu = 1.865 \cdot 10^{-5} \left(\frac{T}{T_0} \right)^{0.7} \tag{1}$$

$$\lambda = 0.144 \cdot (1 + 2.7 \cdot 10^{-9} p) \left(\frac{T}{T_0} \right)^{0.71 \cdot (1 - 2 \cdot 10^{-9} p)} \tag{2}$$

in which T is the temperature of helium in kelvin ($T_0 = 273$ K), while p is helium pressure in pascal. The relation between the Prandtl number and the dynamic viscosity and thermal conductivity is described by the formula:

$$\mathrm{Pr} = \frac{c_p \mu}{\lambda} \tag{3}$$

where c_p is the specific heat of helium.

According to [11], specific heat is equal to 5195 J/(kg K). It changes very little with temperature and pressure (it increases slightly with pressure and decreases with temperature), therefore a constant value of this parameter will be used.

3.2. Heat exchange between the sphere surface and the cooling gas – heat transfer coefficient

Taking into account the high mass flow of the coolant, one can assume that the convection of heat from the spheres to the helium dominates over other heat dissipation mechanisms. Heat transfer during forced heat convection is a complex process, which depends on many factors, such as: the velocity and direction of the coolant relative to the cooled object, the parameters of the fluid (density, viscosity, thermal conductivity), as well as the shape and size of the object itself. The amount of the heat energy collected by the helium flowing past the spheres can be estimated via the Nusselt number (Nu), which in turn can be calculated from an empirical formula that relates it to the Reynolds and Prandtl numbers. In the present calculations the following formulas, applicable to a porous medium (which is typically used for modelling packed beds), are used [4]. For the reduced Reynolds number

$$\mathrm{Re} = \frac{u_{sf} d}{\nu} \tag{4}$$

in which: u_{sf} is the superficial velocity (the product of local velocity u and the porosity ϵ of the packed bed) of flowing helium, ν is its kinematic viscosity and d is the diameter of a sphere. The Nusselt number can be obtained using a Wakao-type expression for a porous medium, given by the formula:

$$\mathrm{Nu} = 2 + 1.1 \cdot \mathrm{Pr}^{1/3} \cdot \mathrm{Re}^{1/2} \tag{5}$$

From the definition of the Nusselt number the heat transfer coefficient h $\left[\mathrm{W/(m^2\,K)}\right]$ is equal to:

$$h = \frac{\lambda \mathrm{Nu}}{d} \tag{6}$$

Since the heat transfer coefficient as well as the dynamic and kinematic viscosity of helium tend to change with pressure and temperature, while the Reynolds number depends on the velocity of helium flow at a given location, the heat transfer coefficient h as calculated from Eq. (6) depends on the location inside the target.

3.3. Equation governing the temperature of the spheres

The absorption of beam energy by the spheres takes place during a very short time of a beam pulse, at the beginning of each energy release cycle. The heat energy is absorbed by the whole volume of the spheres.

Afterwards, during the rest of the cycle t_c, the heat energy is being transferred to the helium flowing past the spheres. It is to be expected that the part of a sphere closest to its surface will cool faster than the one near the centre. The cooling of the outer layer of a sphere as a result of the heat transfer from the sphere to the coolant is accompanied by the process of heat conduction from the centre of the sphere towards its outer regions. The combination of both these processes is accounted for by the Biot number [4], defined by the formula:

$$\mathrm{Bi} = \frac{h}{\lambda_{Ti}} \cdot \frac{V_s}{A_s} \tag{7}$$

in which λ_{Ti} is the thermal conductivity of titanium, h is the heat transfer coefficient between a sphere and the cooling gas, V_s is the volume of a sphere and A_s its surface. When the calculated Biot number is much lower than one, the total heat-transfer resistance is dominated by the resistance to the heat flow between the surface of the sphere and helium. For this reason the temperature distribution inside the sphere tends to be essentially uniform. Under the assumption that the heat transfer coefficient does not exceed 5000 W/(m^2 K), the Biot number is less than 0.11, therefore the temperature distribution inside the spheres will be nearly uniform. In order for the Biot number to be equal to one, the heat transfer coefficient h between the spheres and helium would need to reach the value of 43 800 W/(m^2 K).

The heat energy released from the surface of the spheres and that introduced into the cooling gas during a small time interval dt are in balance. Considering a small element dV of the target, the following equation holds:

$$dm \cdot c_s \cdot dT_s = -\left(T_s - T\right) \cdot dS \cdot h \cdot dt \tag{8}$$

where: T_s is the temperature of a sphere, T is the cooling gas temperature, c_s stands for the specific heat of the spheres, h - heat transfer coefficient between the sphere surface and the coolant, dm, dS - total mass and surface of the spheres in element dV, respectively. The temperature of the spheres T_s and the temperature of gas T are functions of time and coordinates describing the location inside the target.

The differential equation that defines the temperature of the spheres is given as follows:

$$\tau_0 \frac{\partial T_s}{\partial t} + T_s = T \tag{9}$$

$$\tau_0 = \frac{\rho_s c_s d}{6h} \tag{10}$$

Here, ρ_s is the mass density of the spheres.

During the steady-state operation of the target the temperature change of the cooling gas with time is insignificant (small fluctuations that take place within each cycle can be disregarded). Therefore, the gas temperature T can be approximated by its time-average T_a. The solution of the differential equation (9) under steady-state operation is:

$$T_s = T_a + \left(\left(T_s\right)_{max} - T_a\right) \exp(-t/\tau_0) \tag{11}$$

where: $\left(T_s\right)_{max}$ - temperature of a sphere at $t = 0^+$ directly after the beam impact, at the beginning of each cycle.

3.4. Energy deposition inside the target

Energy is deposited inside the spheres non-uniformly throughout the target volume. The most energy is deposited in the immediate vicinity of the target axis and it decreases with the distance from the axis. A decrease in energy also takes place along the axial coordinate z (Fig. 1). Based on the results obtained with FLUKA, the distribution of the average beam power density inside the target can be approximated for the purpose of the following analysis by a function:

$$G(x,y,z) = \begin{cases} a_0 e^{-\frac{1}{2}\frac{x^2+y^2}{\sigma^2}} \left(b_0 + b_1 z + b_2 z^2 + b_3 z^3 + b_4 z^4\right), & \text{for } z \le 0.08\,\mathrm{m} \\ a_0 e^{-\frac{1}{2}\frac{x^2+y^2}{\sigma^2}} \left(c_0 + c_1 z + c_2 z^2 + c_3 z^3 + c_4 z^4\right), & \text{for } z \ge 0.08\,\mathrm{m} \end{cases} \tag{12}$$

Table 1
Parameters of the power density function.

Parameter	Value	Parameter	Value
a_0	1.057×10^9 [W/m^3]		
b_0	1.806 [–]	c_0	2.320 [–]
b_1	42.35 [1/m]	c_1	−1.871 [1/m]
b_2	−1386 [1/m^2]	c_2	−10.88 [1/m^2]
b_3	18 410 [1/m^3]	c_3	21.83 [1/m^3]
b_4	−89 190 [1/m^4]	c_4	−11.98 [1/m^4]

Table 2
Power deposition inside individual sectors of the target.

Sector number	Sector coordinates: z_1–z_2 [m]	Power [kW]
I	0–0.08	28.49
II	0.08–0.18	31.76
III	0.18–0.28	25.39
IV	0.28–0.38	19.09
V	0.38–0.48	13.68
VI	0.48–0.58	9.52
VII	0.58–0.68	6.50
VIII	0.68–0.78	4.03
Total	0–0.78	138.46

in which $\sigma = 0.005$ m, while the values of the remaining parameters are listed in Table 1.

Power density function $G(x,y,z)$ $\left[\mathrm{W/m^3}\right]$ introduced above specifies the power deposited by the beam per unit volume of the target. However, the energy is stored in the spheres, which occupy only partially the volume of the target. Therefore, it is convenient to introduce specific energy q $\left[\mathrm{J/kg/cycle}\right]$, the amount of energy deposited in 1 kg of sphere material during one cycle of operation. The value of q can be calculated from the power density function using the formula:

$$q(x,y,z) = G(x,y,z)\frac{1}{\beta_V \rho_s f} \tag{13}$$

where β_V is the sphere packing ratio.

In order to reduce the scope of the problem and to facilitate the calculations, the target is subdivided into several sectors of 10 cm length, except the first one, the length of which will be taken to be 8 cm. Table 2 lists the values of power deposited in each sector, defined by coordinates z_1 and z_2, as well as the total power inside the target.

In addition, in the analytical model and in comparing the Fluent 3D results with those obtained from the one-dimensional analytical model, a power density function $\tilde{G}(y)$ $\left[\mathrm{W/m}\right]$ vs. the transverse coordinate y will be used:

$$\tilde{G}(y) = \int_{z_1}^{z_2} \int_{-\sqrt{D_t^2/4-y^2}}^{\sqrt{D_t^2/4-y^2}} G(x,y,z)\,dx\,dz \tag{14}$$

3.5. Coolant heat balance

During the steady-state operation of the target a balance is established between the heat energy transmitted from the proton beam to the spheres and the increase of the enthalpy of the gas flowing through the target, during the cycle t_c of heat exchange. Thus all the energy from the beam in the period t_c is eventually transmitted through the spheres to the cooling gas. It has been pointed out in Section 3.3 that the fluctuation of the sphere temperature in relation to the average temperature is small. From the point of view of heat transfer the spheres can be considered as a sub-system that averages and redistributes the heat energy provided by proton beam pulses.

The following equations will be used to model the cooling gas [12–14]: equation of conservation of momentum (taking into account the flow resistance due to the packed bed [5,6]):

$$\frac{dp}{dy} = -\rho u \frac{du}{dy} - \left(\frac{\mu}{\alpha} + \frac{1}{2}\rho C_2 |u_{sf}|\right) u_{sf} \tag{15}$$

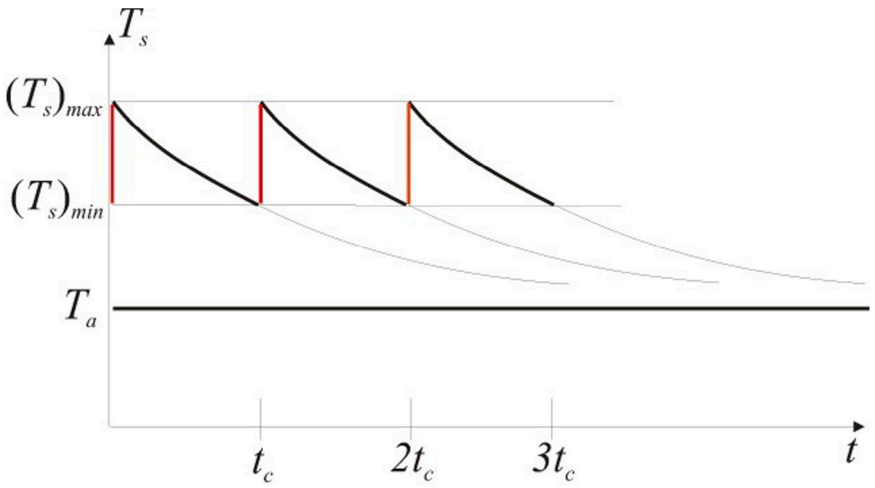

Fig. 2. Graph of sphere temperature T_s and average temperature T_a of flowing gas change during a steady-state operation of the target (red — heating, black — cooling).

ideal gas law:

$$p = \rho R T_a \tag{16}$$

equation of conservation of mass:

$$\rho A_{ef}(y) u = \dot{m} \tag{17}$$

specific heat capacity equation:

$$c_p \frac{dT_{a0}}{dy} = \frac{1}{\dot{m}} \tilde{G}(y) \tag{18}$$

Here: ρ is the gas density, T_a - average temperature of the flowing gas, u - average local velocity and T_{a0} - stagnation temperature. Additionally, A_{ef} represents the effective cross-section area through which the flow of cooling gas takes place, R [J/(kg K)] is the individual gas constant for helium, while $\dot{m}$ [kg/s] - mass flow rate of the helium passing through the target.

Eq. (15) is valid under the assumption that the spheres packed in the target can be modelled by a corresponding homogeneous isotropic porous medium of porosity $\epsilon = 1 - \beta_V$. The additional term on the right-hand side of Eq. (15) represents the resistance of the porous medium to gas flow, due to both viscous and inertial losses. The value of permeability α [m^2] and the inertial loss coefficient C_2 [1/m] can be determined using the following formulas:

$$\alpha = \frac{d^2}{150} \frac{\epsilon^3}{(1-\epsilon)^2}, \; C_2 = \frac{3.5}{d} \frac{(1-\epsilon)}{\epsilon^3} \tag{19}$$

The velocity u_{sf} in Eq. (15) is the so-called superficial velocity, which is related to the average local velocity u by the formula $u_{sf} = \epsilon u$.

The stagnation temperature T_{a0} depends on the temperature T_a of the flowing gas through the formula:

$$T_{a0} = T_a \left(1 + \frac{\kappa - 1}{2} \mathrm{Ma}^2\right) \tag{20}$$

where Ma is the Mach number:

$$\mathrm{Ma} = \frac{u}{\sqrt{\kappa R T_a}} \tag{21}$$

The specific heat ratio κ of helium is equal to 5/3.

3.6. Steady-state operation of the target

In order for the target to operate in a steady-state condition, the heat energy transmitted from the beam to the spheres and the heat energy transferred from the spheres to helium must be balanced over each period t_c. This condition can be written as:

$$(T_s)_{max} - T_s(t_c) = \Delta T_s \tag{22}$$

where ΔT_s is the sphere temperature increase due to a short beam pulse at the beginning of each cycle. The increase in the temperature is equal to:

$$\Delta T_s = \frac{q}{c_s} \tag{23}$$

in which c_s is the specific heat of the material of the spheres, while q is the energy transmitted at the beginning of each cycle from the beam to 1 kg of spheres. The increase in temperature ΔT_s and specific energy q (Eq. (13)) depend on the position inside the target.

By combining the steady-state condition given by Eq. (22) with Eq. (11) describing the temperature of the spheres, one obtains the formulas that determine the maximal and minimal temperature of the spheres in steady-state operation:

$$\begin{aligned} (T_s)_{min} &= T_a + \frac{\exp(-t_c/\tau_o)}{1 - \exp(-t_c/\tau_0)} \Delta T_s \\ (T_s)_{max} &= T_a + \frac{1}{1 - \exp(-t_c/\tau_0)} \Delta T_s \end{aligned} \tag{24}$$

The graph representing the sudden increase in the temperature T_s of a given sphere and its subsequent decrease, as obtained from Eqs. (11) and (24), is shown schematically in Fig. 2. The average temperature T_a of the flowing gas is also shown.

4. Results of calculations

The main focus of the calculations has been placed on the first sector (Table 2) of the target, in which the most energy will be deposited during target operation.

In accordance with the discussion and equations of the previous chapters, the calculations can be performed in two stages. In the first stage the focus is placed on calculating the parameters of the cooling gas, while in the second — on the temperature of the spheres inside the target. The calculation of the gas parameters is done by solving the system of Eqs. (15)–(18), after the preliminary introduction of Eqs. (1), (19) and formula $u_{sf} = \epsilon u$ into Eq. (15) and at the same time Eqs. (14), (20), (21) into Eq. (18). Data used in the calculations have been collected in Appendix. The parameters of the gas sought are: pressure $p(y)$, temperature $T_a(y)$, velocity $u(y)$ and density $\rho(y)$.

The calculations of the sphere temperature, performed in the second stage, utilize the results obtained in the previous step. These calculations consist in determining the heat transfer coefficient h, using Eq. (6) with the introduction of Eqs. (1)–(5), and then calculating the time constant τ_o using Eq. (10), and finally obtaining the minimal temperature $(T_s)_{min}$ and maximal temperature $(T_s)_{max}$ of the spheres from Eq. (24). All results obtained in the second stage are functions of y.

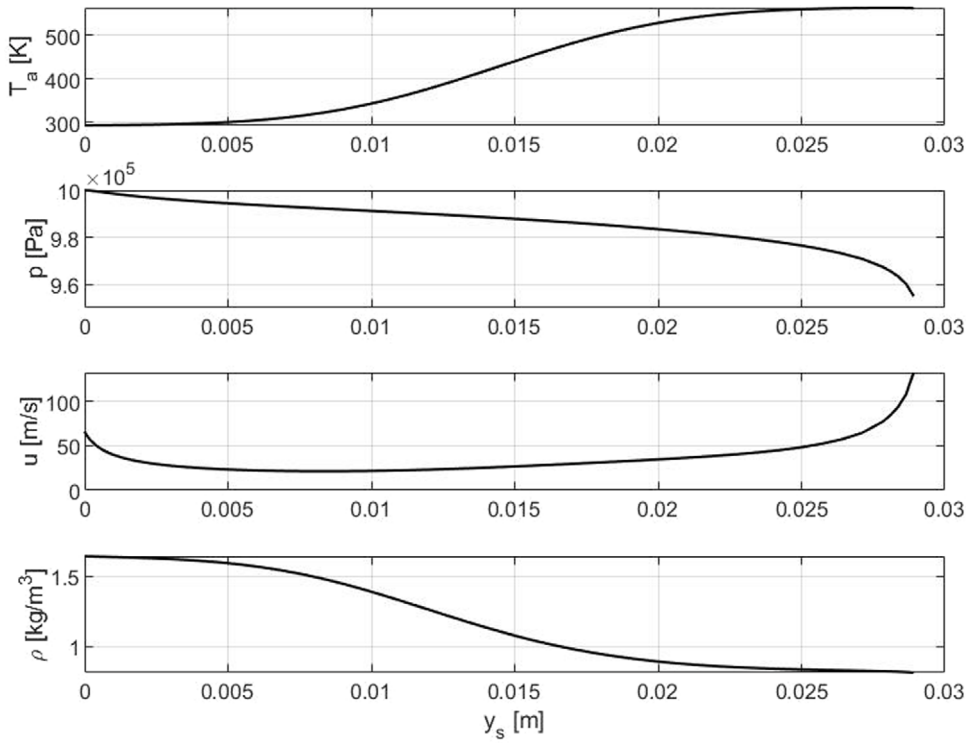

Fig. 3. Helium flow parameters obtained from the analytical approach for transverse flow (first sector).

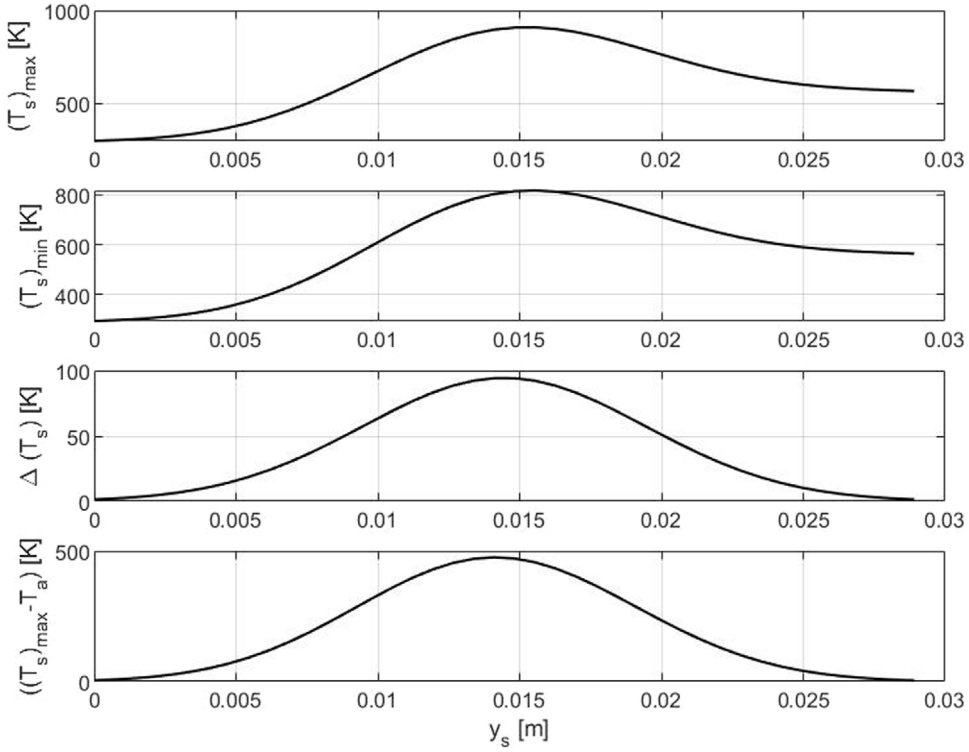

Fig. 4. $(T_s)_{max}$, $(T_s)_{min}$ and ΔT_s of the spheres in each beam cycle (first sector).

Fig. 3 presents the temperature T_a, pressure p, velocity u and density ρ of helium within the first target sector, plotted against transverse local co-ordinate y_s measured with respect to the location of the inlet slot. The results of calculating the sphere temperatures $(T_s)_{max}$, $(T_s)_{min}$ and ΔT_s are shown in Fig. 4.

In addition to the analytical model discussed, a CFD model has been prepared using the ANSYS Fluent package. Whereas with the analytical solution it is possible to determine both the parameters of the gas and the temperature of the spheres, the CFD approach is limited to the parameters of the gas.

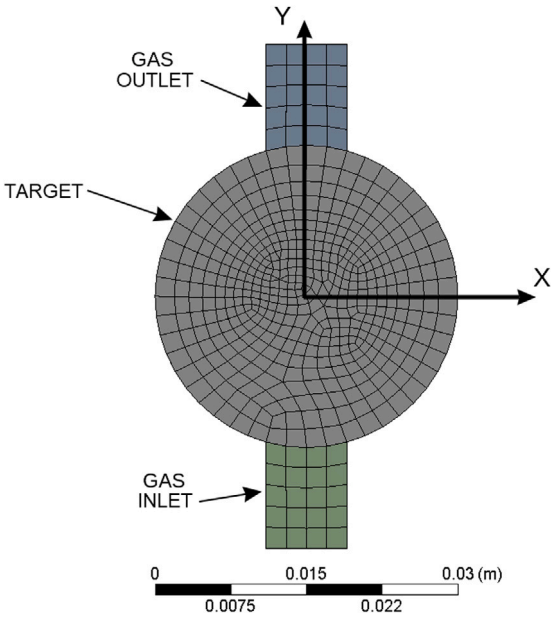

Fig. 5. 2D mesh used in the CFD analysis of transverse helium flow through the granular target, with regions corresponding to the target, the inlet and the outlet slot.

In the CFD simulations it has been assumed that the porous medium in question is homogeneous and isotropic, in which case the flow resistance force (per unit volume) in the packed bed is expressed by formula [15]:

$$F_i = -\left(\frac{\mu}{\alpha}\left(u_{sf}\right)_i + C_2\frac{1}{2}\rho|u_{sf}|\left(u_{sf}\right)_i\right), \quad i = x, y, z \tag{25}$$

The helium and target parameters and data used in the calculations have been grouped in Appendix. In the CFD simulations dynamic viscosity had to be assumed to be constant ($\mu = 1.99 \times 10^{-5}$ Pa s).

The boundary conditions for the CFD analysis have been defined by specifying the pressure inlet at gauge pressure $p_{gp} = 0$ bar and absolute operating pressure $p_{op} = 10$ bar. The helium inlet temperature has been assumed to be equal to 293 K.

Fig. 5 shows the plane mesh of the target cross-section used in the numerical analysis of the transverse helium flow, with specific zones corresponding to the target and the inlet and the outlet slots. This mesh has then been expanded along the target length to obtain a volumetric mesh of a 3-D model.

Fig. 6 shows the results of the CFD analysis using the ANSYS Fluent software, under the steady-state condition, for helium global mass flow $\dot{m} = 200$ g/s (mass flow for the whole target) and the beam power distribution inside the target as specified earlier in Section 3.4. As a result of the symmetry of the problem all the plots in Fig. 6 display symmetry with respect to the yz plane — all quantities are described by even functions of the x-coordinate. Along the z-axis the profiles shown appear similar. However, since the most proton beam power is dissipated in the initial part of the target, the temperature tends to decrease with the z-coordinate, after the first sector.

As can be seen from both the analytical and the CFD simulations, the velocity of the flowing gas decreases in the vicinity of the target axis, where the beam power density is the highest, and it increases at the outlet (Figs. 3, 6a). The decrease in the gas velocity in the region close to the target axis results in a significant reduction in the heat transfer

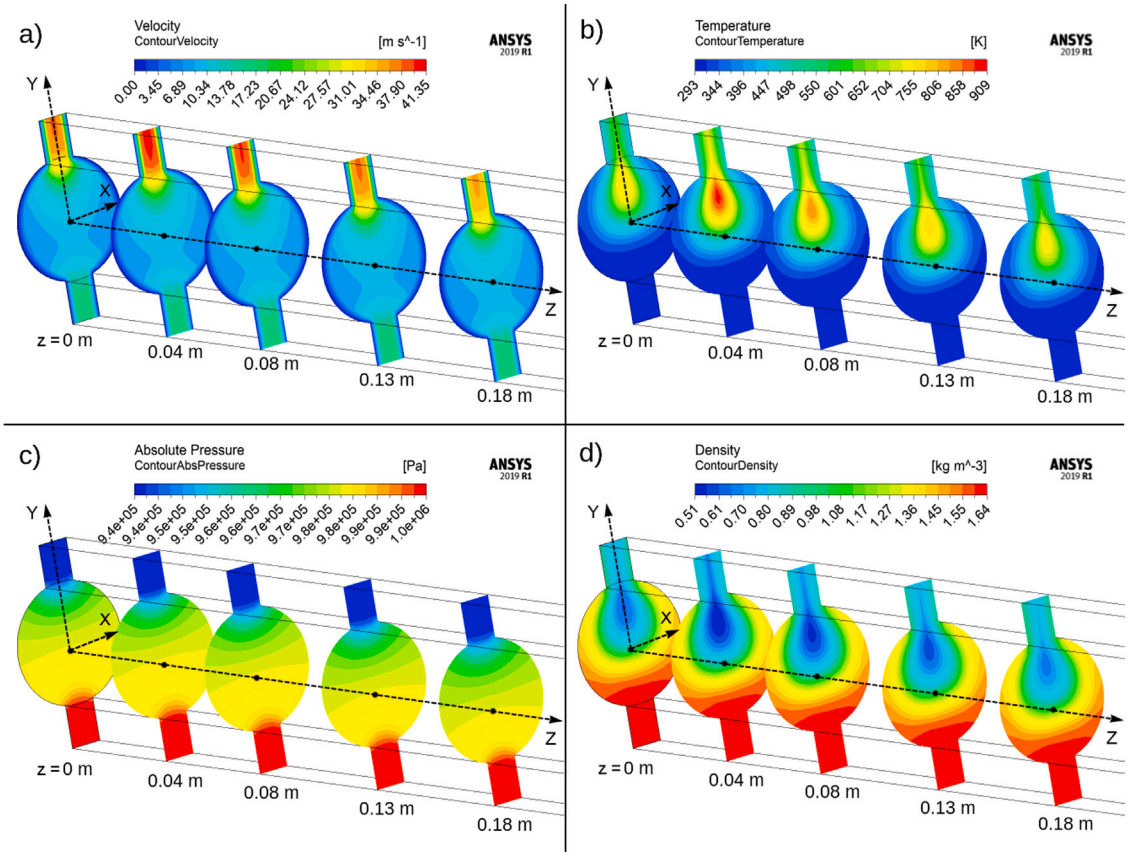

Fig. 6. Distribution of superficial velocity [m/s] (a), temperature [K] (b), absolute pressure [Pa] (c) and density [kg/m^3] (d) of helium flowing upwards in transverse direction through the first two sectors of the target under constant helium mass flow 200 g/s and non-homogeneous power deposition inside the target of total value $\dot{Q}$ =138.53 kW.

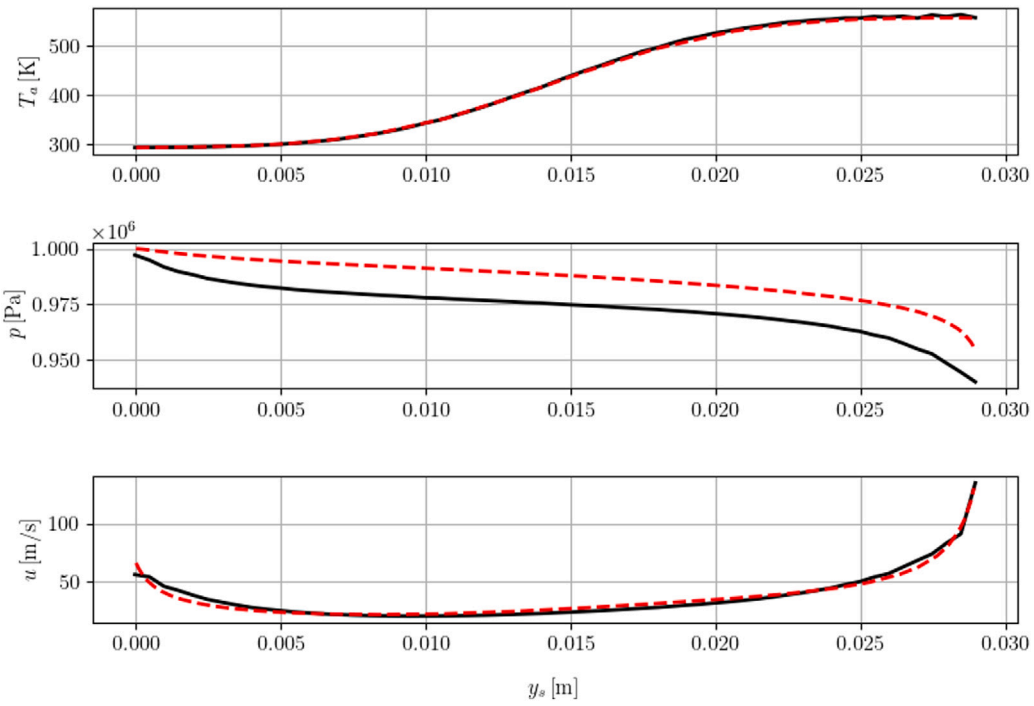

Fig. 7. Mass weighted average for helium flow parameters obtained for the transverse flow (first sector) from the analytical solution (red dashed lines) and the numerical solution (black solid lines).

coefficient in this region, which in turn decreases the heat exchange between the spheres and the gas. As a result, there is a considerable increase in the temperature of the spheres in this region, which can be seen in Fig. 4.

The maximum temperature of the spheres is approximately 800 K, much lower than the melting point of titanium (approx. 2000 K). Therefore helium cooling is efficient enough to keep the temperature at an acceptable level, so that the possibility of titanium melting is avoided.

When comparing the velocities obtained from the analytical and CFD computations it is important to bear in mind that the latter uses superficial velocity $u_{sf} = \epsilon u$. When the re-calculation is performed to obtain the value of the local velocity, the results obtained from both approaches are comparable. It needs to be pointed out that the maximal velocity of the gas is much lower than the velocity of sound in helium under the same conditions (maximum value of Mach number $\mathrm{Ma}_{max} \approx 0.2$). The gas density is found to decrease about two times during the flow across the target.

In order to describe the target cooling system under consideration, the values of temperature, pressure and flow velocity are of particular importance. Fig. 7 shows the graphs of the mass-weighted average temperature, pressure and velocity of helium inside the first sector of the target obtained from the CFD results in comparison to the corresponding results obtained via the analytical approach, previously presented in Fig. 3.

The calculations have focused on the first sector of the target, in which the most of the beam energy is deposited. The biggest difference between the results exists for the gas pressure, the CFD simulations resulting in a higher gas pressure drop between the inlet and the outlet. This discrepancy is mostly due to different assumptions about the viscosity of helium used in the two models. The results obtained for the temperature and velocity from the CFD and analytical approach agree well.

5. Conclusions and further considerations

The paper has discussed two approaches to solving the problem of a compressible gas flow through a granular target, combined with convective heat transfer. In the analytical approach the heat transfer and fluid mechanics equations were used to determine the transfer of heat at all stages, from the proton beam impact, through the spheres and then to the cooling gas. As for the calculation performed using the CFD approach, it was assumed that the heat was transmitted directly from the proton beam to the gas flowing through the target, omitting the sphere heating. In both cases, the granular target was modelled by a porous medium in order to simplify the calculations. The results were obtained for the temperature, pressure, velocity and density distribution of helium inside the target.

Both the analytical and the CFD calculations have been performed with a realistic energy distribution, by using the power distribution function obtained by fitting the values obtained with the FLUKA software for the future ESSνSB conditions. The results of the analytical and the CFD analyses are very comparable, showing that the analytical model can be used instead of the computationally more expensive CFD approach in the evaluation of target cooling. The analysis has shown that it is feasible to utilize gaseous helium to effectively cool down a granular target, in which very high power is deposited by the impinging proton beam. Both analyses have considered cooling under a steady-state condition. No gradual increase of the temperature of the spheres under subsequent beam pulses has been dealt with in this paper.

Declaration of competing interest

The authors declare that they have no known competing financial interests or personal relationships that could have appeared to influence the work reported in this paper.

Acknowledgements

This study has received funding from the European Union's Horizon 2020 research and innovation programme under grant No 777419 (ESSνSB)

This scientific work has received funding from the Polish Ministry of Science and Higher Education, Poland, grant No W129/H2020/2018,

from the science resources for the years 2018–2021 for the realization of a co-funded project

The authors express their gratitude to Dr Loris D'Alessi for providing the map of energy deposition by a proton beam, calculated for the needs of the future ESSνSB experiment.

Appendix. Summary of parameters and data used in the calculations

Gaseous helium	
Individual gas constant R	2079 J/(kg K)
Specific heat capacity c_p	5195 J/(kg K)
Specific heat ratio $\kappa = c_p/c_v$	5/3
Inlet parameters of helium	
Operational pressure p_{op}	1×10^6 Pa = 10 bar
Temperature T	293 K
Density ρ	1.64 kg/m^3
Velocity u	66 m/s
Mach number Ma	0.066
Mass flow $\dot{m}_p$	0.2 kg/s
Superficial velocity u_{sf}	19.8 m/s
Target (packed bed)	
Length L_t	0.78 m
Diameter D_t	0.03 m
Average volume packing ratio β_V	0.66
Width of inlet and outlet slot b_t	0.008 m
Titanium spheres	
Diameter d	0.003 m
Density ρ_s	4500 kg/m^3
Specific heat capacity c_s	600 (J/kg K)
Porous medium	
Permeability α	5.4×10^{-9} m^2
Viscous resistance $1/\alpha$	1.85×10^8 1/m^2
Inertial resistance C_2	1.96×10^4 1/m
Porosity $\epsilon = 1 - \beta_V$	0.34
Proton beam	
Pulse repetition frequency f	14 Hz
Period of one cycle t_c	0.07143 s
Energy transmitted to spheres has been specified in Section 3.4	

References

[1] P. Sievers, A Stationary Target for the CERN-Neutrino-Factory, CERN, 2001, CERN-NuFact-Note 065.
[2] E. Baussan, et al., Neutrino super beam based on a superconducting proton linac, Phys. Rev. Spec. Top. - Accel. Beams 17 (3) (2014) 031001.
[3] E. Baussan, et al., A very intense neutrino super beam experiment for leptonic CP violation discovery based on the European spallation source linac, Nuclear Phys. B 885 (2014) 127–149.
[4] E. Achenbach, Heat and flow characteristics of packed beds, Exp. Therm. Fluid Sci. 10 (1) (1995) 17–27.
[5] S. Ergun, A.A. Orning, Fluid flow through randomly packed columns and fluidized beds, Ind. Eng. Chem. 41 (6) (1949) 1179–1184.
[6] S. Ergun, Fluid flow through packed columns, Chem. Eng. Prog. 48 (1952) 89–94.
[7] S. Prager, Viscous flow through porous media, Phys. Fluids 4 (12) (1961) 1477–1482.
[8] M. Winterberg, E. Tsotsas, Modelling of heat transport in beds packed with spherical particles for various bed geometries and/or thermal boundary conditions, Int. J. Therm. Sci. 39 (2000) 556–570.
[9] O. Kovalev, A. Gusarov, Modeling of granular packed beds, their statistical analyses and evaluation of effective thermal conductivity, Int. J. Therm. Sci. 114 (2017) 327–341.
[10] C. Du Toit, P. Rousseau, G. Greyvenstein, W. Landman, A systems CFD model of a packed bed high temperature gas-cooled nuclear reactor, Int. J. Therm. Sci. 45 (2006) 70–85.
[11] H. Petersen, The Properties of Helium: Density, Specific Heats, Viscosity, and Thermal Conductivity at Pressures from 1 to 100 Bar and from Room Temperature to About 1800 K, Report No. 224, Danish Atomic Energy Commission Risø, 1970.
[12] Y. Nakayama, R. Boucher, Introduction to Fluid Mechanics, Elsevier, 1998.
[13] L.D. Landau, E.M. Lifshitz, Fluid Mechanics: Volume 6 (Course of Theoretical Physics), second ed., Butterworth-Heinemann, 1987.
[14] R.L. Daugherty, J.B. Franzini, Fluid Mechanics with Engineering Applications, seventh ed., McGraw-Hill Kogakusha, Tokyo, 1977.
[15] ANSYS Fluent Theory Guide, Release 15.0, ANSYS Inc., 2013.